Integrated Approach to Assess the Resilience of Future Electricity Infrastructure Networks to Climate Hazards

Gaihua Fu, Sean Wilkinson, Richard J. Dawson, Hayley J. Fowler, Chris Kilsby, Mathaios Panteli, *Member, IEEE*, and Pierluigi Mancarella, *Senior Member, IEEE*

***Abstract*—Electricity systems are undergoing unprecedented change, with growing capacity for low-carbon generation, and an increasingly distributed approach to network control. Furthermore, the severity of climate related threats is projected to increase. To improve our understanding of the risks from these changes, this paper presents a novel modeling approach to assess the resilience of future electricity networks to climate hazards. The approach involves consideration of the: 1) evolution of electricity networks in response to changes in demand, supply, and infrastructure development policies; 2) implication that these policies have on network configuration and resilience; and 3) impacts of potential changes in climate hazard on network resilience. We demonstrate the research on the National Electricity Transmission System of Great Britain and assess the resilience of this system to changes in the intensity of wind storms under alternative energy futures. The analysis shows that infrastructure policies strongly shape the long-term spatial configuration of electricity networks and consequently this has profound impacts on their resilience. Though the system is resilient to wind storms under the current climate, our analysis shows that the system fails to meet electricity demand after an increase of only 5–10% in the intensity and frequency of wind storms, and a 50% increase could lead to the loss of 85% of peak winter demand. The approach is useful for identifying and communicating potential network risks to wider stakeholders and policy makers seeking to design a transition toward a low-carbon, yet resilient, future electricity systems.**

***Index Terms*—Complex system modeling, climate change, electricity networks, infrastructure resilience, resilience assessment.**

Manuscript received November 18, 2016; revised April 15, 2017; accepted April 23, 2017. Date of publication May 19, 2017; date of current version November 22, 2018. This work was supported in part by the U.K. Natural Environment Research Council under Grant NE/N012852/1, in part by the Engineering and Physical Sciences Research Council under Grant EP/I035781/1 and Grant EP/K012398/1, and in part by the European Commission Seventh Framework Programme grant (Project Reference: 265240). The work of H. J. Fowler was supported in part by the Wolfson Foundation and in part by the Royal Society as a Royal Society Wolfson Research Merit Award (WM140025) holder. *(Corresponding author: Gaihua Fu.)*

G. Fu is with the National Grid plc, Reading RG41 5BN, U.K. (e-mail: Gaihua.Fu@nationalgrid.com).

S. Wilkinson, R. J. Dawson, H. J. Fowler, and C. Kilsby are with the School of Civil Engineering and Geosciences, Newcastle University, Newcastle upon Tyne NE1 7RU, U.K. (e-mail: Sean.Wilkinson@ncl.ac.uk; Richard.Dawson@ncl.ac.uk; Hayley.Fowler@ncl.ac.uk; Chris.Kilsby@ncl.ac.uk).

M. Panteli and P. Mancarella are with the School of Electrical and Electronic Engineering, University of Manchester, Manchester M13 9PL, U.K. (e-mail: mathaios.panteli@manchester.ac.uk; p.mancarella@manchester.ac.uk).

Digital Object Identifier 10.1109/JSYST.2017.2700791

I. Introduction

ELECTRICITY systems are a key element of the critical infrastructure of a modern society [1]–[3]. Reliable operation of electricity systems is being challenged from several fronts. First, electricity systems are changing rapidly as a result of the closure of many fossil fuel plants, the increased use of low-carbon generation, and the deployment of smart grid technologies. Second, electricity demand is expected to increase as a result of the electrification of heating and transport systems. This will change demand profiles, with daily peaks and troughs likely to become exacerbated [4]. These changes not only introduce complexities for system operation but, in many situations, may require changes to the network architecture which, in turn, can alter the reliability and resilience of an electricity system.

Furthermore, predicted changes to the climate are expected to increase the frequency and severity of extreme weather events such as heatwaves, floods, and wind storms [5]–[8]. In comparison to other disruptive events (e.g., equipment failure or malicious attacks), weather-related hazards typically have a larger geographical footprint and hence are more disruptive. In the U.K., weather events are responsible for approximately half of the energy not supplied [9]. In North America, around half of energy supply failures and nearly three quarters of larger failures were caused by weather hazards [10]. Similar results have also been reported in [11] and [12].

The vulnerability of electricity systems has been the subject of past scrutiny [13]–[17], and recently a growing body of literature has sought to assess the resilience of electricity systems to climate change and extreme weather events [18]–[22]. For example, empirical studies [11], [23]–[26] have provided insights into the historical vulnerability of a network to observed weather conditions. Monte-Carlo simulation based approaches have been used to model the stochastic behavior and dynamics of electricity systems during disruptive events [17], [27]–[29]. However, most previous research has used artificial or simplified network structures (e.g., IEEE bus-bar models) or transformed an electricity system into a simplified form. The methods have been rarely applied to assess the vulnerability and resilience of large real-world electricity infrastructures to extreme weather events. Furthermore, little consideration has been given to the uncertainties and risks to the resilience of electricity systems arising from infrastructure policies and changes to infrastructure networks.

To improve the understanding of how uncertainties associated with future climate may affect electricity systems, and how

infrastructure development policies can better support the management of system risks, this research proposes an integrated modeling framework for assessing the resilience of future electricity systems under climate hazards. The framework couples simulations of a network growth model, a climate hazard model, a fragility model, and a time series analysis model, with the aim of exploring the following:

1) how electricity networks may evolve in response to changes in demand, supply, and infrastructure policies;
2) how different network evolutionary pathways might impact on the resilience of electricity systems;
3) how potential changes in the severity of climate-related hazards may impact on network resilience.

This proof-of-concept study is implemented on the national electrical transmission system of Great Britain (GB).

Compared to previous work, a number of advances have been made. First, previous research focuses only on the vulnerability of current electricity networks [14], [17], [20], [21] and does not consider uncertainties and risks from future development and changes. By incorporating a network growth model into the framework, we have simulated the evolution of an electricity network under different infrastructure policies and explored the resilience implications of these policies. Second, assessments usually assume that a network component has a constant failure rate for a given weather condition [16], [21]. Here, a fragility approach, which better reflects the stochastic behavior of real systems, has been employed to investigate the failure probability of a network component. Finally, previous research analyses the climate resilience of electricity networks using simplified weather classifications, e.g., by dividing the embedded space of an electricity system into a small number of weather zones, and components within a zone are assumed to experience same weather conditions [28]. This paper has used a high-resolution simulation method to generate time series of weather hazards simultaneously at multiple locations, enabling a more realistic assessment of spatially varying hazard properties.

The results serve as a useful means for communicating potential network risks to wider stakeholders and policy makers in their decisions toward adapting electricity networks to ensure not only the security of electricity supply but also meet decarbonization objectives. Following this introduction, Section II describes a spatial network model to simulate the growth of electricity systems in response to socio-economic drivers; Section III describes the integrated modeling approach to assessing the resilience of electricity networks to climate hazards; while Sections IV and V demonstrate the model using a case-study of the GB national transmission network, before the conclusions are summarized in Section VI.

II. Network Growth Modeling

Drawing from complex network theory [30], [31], a model has been developed to represent electricity networks, and to simulate their growth and evolution.

A. Network Modeling

A network is defined here as a pair $G = \{\mathcal{V}, \mathcal{E}\}$, where $\mathcal{V}$ is a set of network nodes (vertices) and $\mathcal{E}$ is a set of edges (links) that connect pairs of nodes in $\mathcal{V}$ and $\mathcal{E} \subset \mathcal{V}X\mathcal{V}$. An electricity system is modeled as a network with two types of nodes, i.e., $\mathcal{V} = \mathcal{V}^G \cup \mathcal{V}^D$, with $\mathcal{V}^G$ as a set of nodes representing power generators that produce the electricity required by consumers, and $\mathcal{V}^D$ as a set of nodes representing electricity substations that transfer electricity among power lines, or transport electricity to customers or systems that satisfy consumer demand. A node in $\mathcal{V}^G$ is defined as $\langle v,\ x_{\mathrm{loc}},\ y_{\mathrm{loc}},\ C^G \rangle$, and a node in $\mathcal{V}^D$ is defined as $\langle v,\ x_{\mathrm{loc}},\ y_{\mathrm{loc}},\ C^D \rangle$, where v is the label of a network node. All nodes are attributed with spatial information x_{loc} and y_{loc} to indicate their geographical location. A node in $\mathcal{V}^G$ has an attribute C^G that indicates the amount of electricity it can generate. A node in $\mathcal{V}^D$ has an attribute C^D that indicates the amount of electricity it supplies to customers or to lower voltage systems, and a node without a customer/lower voltage system connection has $\mathcal{V}^D = 0$. A network link is established between a pair of nodes if there is an electricity line connecting them. An example power network is shown in Fig. 1.

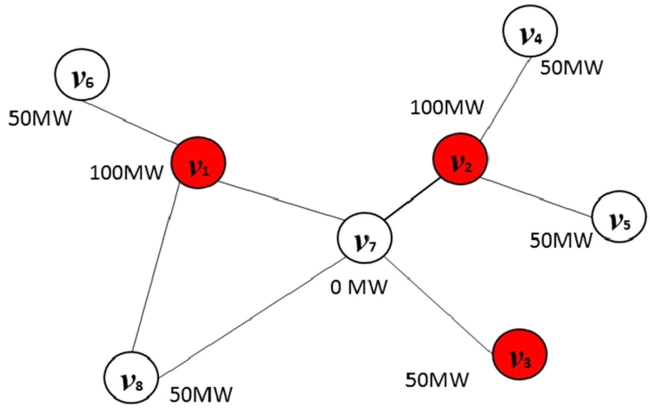

Fig. 1. Network representation of an example electricity system, where red nodes are generators, and others are substation nodes. Links between nodes represent electrical lines/cables. The number next to a node indicates the amount of electricity it generates/supplies.

To ensure the security and reliability of power supply, an electricity system needs to satisfy

$$\sum_{v_i \in \mathcal{V}^G} C_i^G \geq \sum_{v_j \in \mathcal{V}^D} C_j^D. \tag{1}$$

That is, the total amount of available electricity generation is equal or greater than the total amount of electricity demand [32]. Failure of a network component could disconnect a generating node from the system, and therefore reduce the amount of power that the system can generate. A loss of load occurs when the constraint in (1) is violated. For example, if the link $< v_3, v_7 >$ fails in the network illustrated in Fig. 1, the generator v_3 will be disconnected from the system, leading to a loss of load.

B. Network Growth

Electricity networks evolve in response to population growth, new technologies, and policy changes. This evolution can either take the form of re-enforcing existing network components (e.g., by increasing their capacity), or constructing new network components (i.e., nodes and links). The former is relatively easy to model, because the fundamental network topology remains the same and only the capacity attributes of the network components

change. The latter, which is the focus of this work, is relevant to long-term network development and is more complex due to the range of uncertainties associated with long-term change.

The network growth model is built upon our previous research [33], but the key model components are summarized here. Given an initial electricity network *G* (embedded within space *S*), the model evolves *G* into future networks by taking into account the contributions of different drivers of future network growth, including future electricity demand and supply, network wiring practices, and infrastructure development policies. The set of parameters used by the model are listed as follows:

- N_1 the number of new generators to be added to *G*.
- N_2 the number of new substations to be added to *G*.
- $\psi(a)$ the electricity supply density function of *S* in future, and *a* is a subarea of *S*.
- $\phi(a)$ the electricity demand density function of *S* in future, and *a* is a subarea of *S*.
- γ scaling parameter regulating generator distribution.
- δ scaling parameter regulating substation distribution.
- α scaling parameter regulating node linkage.

Spatial distribution of future electricity supply $\psi(a)$ and demand $\phi(a)$, respectively, influences how new generators and substation nodes are allocated in space. The probability of constructing a new generator node *v* in a subarea a of *S* is defined as proportional to the supply density $\psi(a)$ of *a*, i.e.,

$$P\left(v \in \mathcal{V}^G\right) \sim \psi(a)^{\gamma}. \tag{2}$$

Similarly, the probability of constructing a new substation node *u* is proportional to the demand density $\phi(a)$, i.e.,

$$P\left(u \in \mathcal{V}^D\right) \sim \phi(a)^{\delta} \tag{3}$$

where γ and δ are scaling parameters, with the greater the value of γ (or δ), the more likely that *v* is allocated to an area of high electricity supply (or high demand).

A new node connects to *G* by considering network wiring practices and cost, and the efficiency of power flow. The probability $\Pi(\langle v, w\rangle)$ of building an edge $\langle v, w\rangle$ between a new node v and an existing node w is

$$\Pi\left(<v, w>\right) \sim e^{-\frac{d_{v,w}}{\alpha}} \tag{4}$$

where $d_{v,w}$ is the physical distance between *v* and *w*, and α is a scaling parameter introduced to calibrate the connection probability. The smaller the α, the more likely a short link will be established, thereby reducing network construction cost. The larger the α, the more likely a long-range link will be established, facilitating power flow over long distances. New network links are unable to cross an existing link, in line with power industry practice.

Fig. 2 illustrates how the model is used to grow the network shown in Fig. 1. Here, the network is fitted into four demand zones a_{1-4}, and there is an increase of 50 MW of demand in a_1, then a new substation node v_9 is more likely to be constructed within this zone relative to the other zones. However, according to (3), v_9 has a few options to connect to the rest of the network: connecting to v_2 is the most economic choice as it is the closest node to v_9, whilst connecting to v_7 facilitates the use of the surplus electricity in a_3 and a_4, thereby improving flow efficiency. We will demonstrate in Section IV how to configure the model to generate future networks in response to the choices of infrastructure policies.

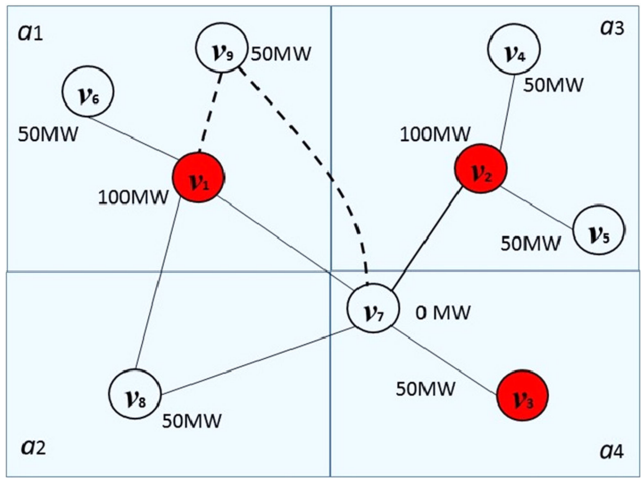

Fig. 2. Illustration of electricity network growth. Demand in area a_1 has increased, and v_9 is introduced to meet this demand increase. It has a few options for network connection, e.g., linkage to v_2 is the most economic, and linkage to v_7 improves flow efficiency.

III. Resilience Assessment of Electricity System Under Climate Hazards

To assess the impacts of climate hazards on the resilience of future electricity networks, an integrated framework has been developed. The framework couples simulations of a climate hazard model, a fragility model, and a time series network analysis model, described as follows.

A. Hazard Modeling

Wind storms have been shown to cause the highest percentage of faults in electricity infrastructure [11] and are therefore used here to demonstrate the resilience framework. This has been achieved using a wind extremes simulator which generates time series of wind gust simultaneously at multiple locations across the U.K. [34]. Historical time series of wind gust from ERA-Interim reanalysis data [35] are used to characterize the space-time properties of extreme events. Storms with statistically similar properties are then simulated at a pressure level of 850 hPa (around 1.5 km above the surface) and at a spatial resolution of 80 km. The wind fields are then downscaled by interpolation to a finer regional model grid of 12 km spatial resolution and converted to surface 3-s gust speed by application of regression models. The output of the simulator is in the form of simultaneous correlated time series of wind gust speed at locations specified by the user (two example wind profiles generated with the simulator are shown in Fig. 3). The simulator reproduces the observed extreme statistics and spatial correlation of extreme winds, by considering seasonal variations in the occurrence of storms throughout the year [see Fig. 4(a)] as well as the seasonally varying lengths and intensities of storm events [see Fig. 4(b)–(d)].

The simulator can generate arbitrarily long time series to enable the analysis of extreme (by definition, infrequently

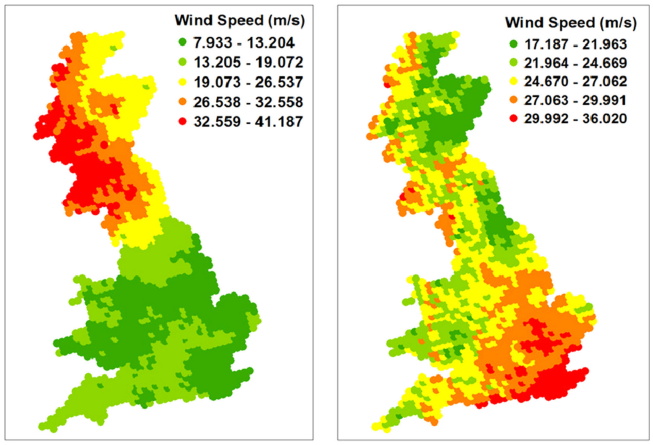

Fig. 3. Two example wind fields generated with the wind simulator showing the spatial variability of storms in Great Britain.

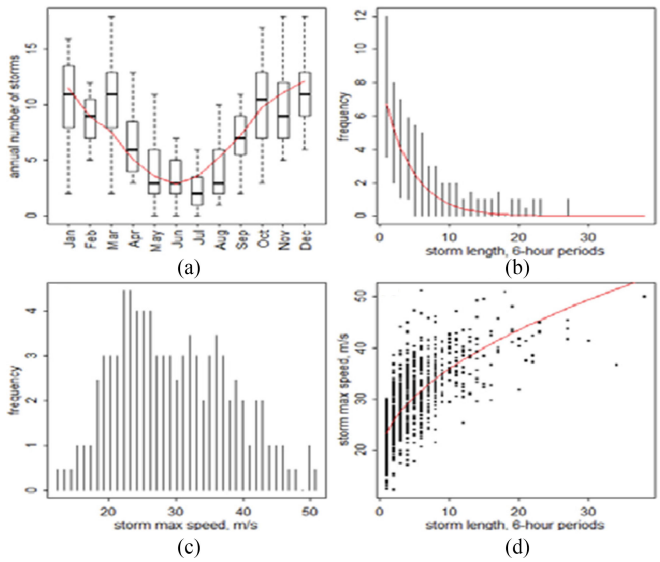

Fig. 4. Distributions of observed storm characteristics (black) showing inter-annual variability over 32 years of record, with fitted statistical model (red line). (a) Annual storm occurrence, (b) storm duration, (c) storm maximum (850 hPa) wind speed, and (d) storm maximum wind speed as a function of storm duration.

occurring) events at a single site, or multisite high wind speeds that have not been observed simultaneously, but are physically possible. Climate models are not yet able to produce reliable projections of future extreme wind statistics because of their coarse grid resolution relative to topographic variability. However, more atmospheric energy associated with climate change is considered likely to increase the intensity and frequency of extreme wind events [36], [37]. Here, the intensity and frequency of wind storms are adjusted to explore the sensitivity to possible future changes.

B. Fragility Modeling of Network Components

The resilience of individual electrical components to wind storm is evaluated through the use of fragility curves. Strong wind causes a number of issues in electricity systems, the most serious being collapse of transmission towers, which are typically distributed at intervals of a few hundred meters along a transmission line. Wind can also directly damage the lines, e.g., through shackle failure, or clashing of conductors or insulators. In the latter cases, wind-related trips might be rectified in a few hours; however, the restoration of an entire tower will take considerably longer. In this study, we only consider the collapse of an entire tower and model its resistance against hazard with a fragility curve [38]–[40], which expresses the failure probability of a tower as a function of wind speed. The shape of the curve depends on the strength of the tower and the variability of the different parameters that contribute to that strength.

A fragility curve can be developed using a number of techniques, ranging from empirical analysis of past events, professional judgment of experienced individuals, analytical methods, or a combination of these. In this study, we have adopted the methodology proposed in [41], which was developed for the Federal Emergency Management Agency to produce fragility curves for seismic hazard. Since there is insufficient data that record wind-related failures of electricity towers in the U.K., an analytical approach was used in this research. Structural models of the L2D towers (the most common tower in the U.K. transmission network) were made using a commercially available structural analysis package. The modeling incorporated a material and geometrically nonlinear analysis to find a wind speed that would result in the collapse of a tower [42]. Uncertainty associated with the different parameters that contribute to structural resistance was considered using the approach described in [41] where uncertainty is described by two factors, namely:

β_γ, which "represents the random variability that is observed in the available test data from which the fragility parameters are determined" and

β_u, which "represents uncertainty that the tests represent the actual conditions of installation and loading that a real component in a building will experience or that the available test data are an inadequate sample to accurately represent the true random variability" [41].

The total uncertainty is the vector sum of the two, i.e.,

$$\beta = \sqrt{\beta\gamma^2 + \beta u^2}. \tag{5}$$

Due to the lack of observational data that can be used to define β_γ, the recommended value of $\beta_u = 0.25$ is adopted by following [41]. This estimate of the uncertainty is likely to lead to conservative strength estimates at low wind speeds and nonconservative estimates at high wind speeds; however, they are unlikely to be greater than the uncertainties relating to future scenarios. The final fragility curve used in this study for the L2D tower is shown in Fig. 5.

C. Time Series Analysis of System Resilience

Wind storms can cover a large geographical area, have peaks of intensity at multiple locations, and wind intensities that vary in time. To assess the impacts of the spatio-temporal variation of wind storms to the resilience of electricity systems, a time series analysis approach is used to assess the resilience of both current and future electricity networks.

At each time step t, a wind storm profile (i.e., the spatial distribution of wind intensity) is generated, and downscaled to

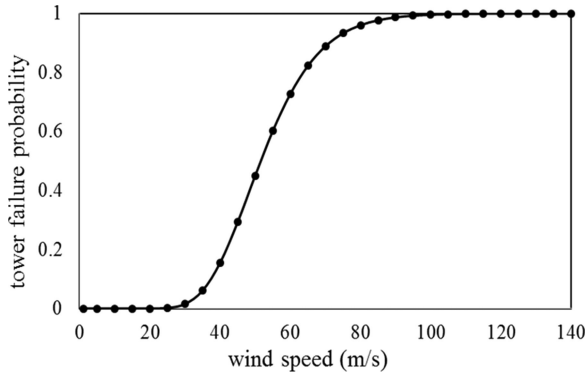

Fig. 5. Fragility curve for L2D towers (which are commonly used in the U.K. transmission network) after [44].

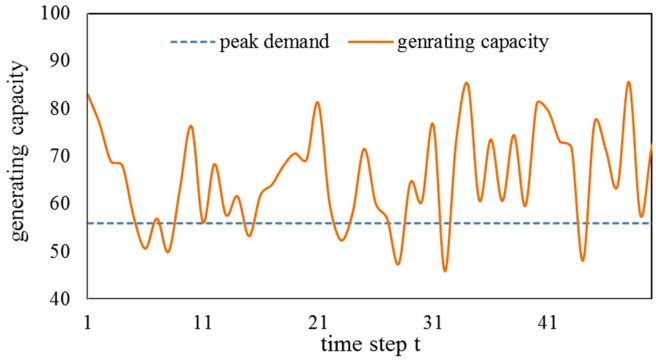

Fig. 6. Illustration of dynamic change of generating capacity and loss of load occurrences for an electricity network.

ground level as described in Section III-A. This is mapped over the electricity network to provide a wind loading at the transmission towers. Using the fragility function in Section III-B, the wind loading is then converted into a failure probability. A line fails if any of its supporting towers collapse and the network link becomes inactive, disconnecting any generation capacity, or removing any associated demand from the system. For computational efficiency, and in line with other large-scale system studies [27], [29], [43]–[45], the remaining connected network components are assumed to operate under all power flow conditions.

A collapsed tower is brought back into the system once it has been repaired. The time required to repair an electricity component usually varies with weather conditions, location, and the time of failure [16], [22], [46]. In this paper, we follow the repair model defined in [16] and [22], but simplify it and only investigate the impacts of weather effects on the repair time of a tower. The time to repair (TTR) of a collapsed tower is determined as a function of wind speed and it increases with wind speed according to

$$\mathrm{TTR} = f_w\left(w\left(t\right)\right) * \mathrm{TTR}_{\mathrm{norm}} \tag{6}$$

where $\mathrm{TTR}_{\mathrm{norm}}$ is the repair time for an electricity tower during normal wind conditions, and is modeled as normally distributed random variables with mean of $\widehat{TTR}_{\mathrm{norm}}$ and $f_w(w(t))$ is a weight factor due to wind which is modeled as

$$f_w\left(w\left(t\right)\right) = \begin{cases} 1, & \text{if } w\left(t\right) < w_{\mathrm{norm}} \\ 1 + \frac{k*(w(t)-w_{\mathrm{norm}})}{\widehat{TTR}_{\mathrm{norm}}}, & \text{if } \left(w\left(t\right) \geq w_{\mathrm{norm}}\right. \end{cases} \tag{7}$$

where $w(t)$ is wind speed at time t, w_{norm} is the wind speed threshold over which TTR is increased, and k is a coefficient for determining how fast that TTR increases with $w(t)$. w_{norm}, $\widehat{TTR}_{\mathrm{norm}}$, and k can be estimated using observed data [16], [22]. With limited published information on past failure incidents of electricity transmission towers in the U.K. that can be used to calibrate these parameters, we have used the values of $\widehat{TTR}_{\mathrm{norm}} = 48\,\mathrm{h}$, $w_{\mathrm{norm}} = 20\,\mathrm{m/s}$, and $k = 2.0$ in our simulation (see Section V), which are comparable to the ones used in [42]. We understand this assumption can introduce inaccuracy in simulation. However, when used consistently, it provides us a useful means to explore the sensitivity of possible future changes to network resilience.

A failed tower is brought back online once its repair time has elapsed, restoring any transmission line and isolated parts of the network, and returning any offline generation capacity. This failure–repair dynamic causes a change in the available generation capacity of the electricity network (see Fig. 6). The generation capacity of the system is evaluated against the system demand at each time step. A loss of load occurrence (LLO) is recorded each time that the generation capacity is below the demand. The demand can either be the daily peak load variation, which includes the peak loads of each day, or the load duration, which represents the hourly variation of the load [47], [48]. However, given the level of uncertainty in estimating the associated parameters in future, it would not be appropriate to express a reliability measure to such a degree of accuracy. As such a single constant peak demand (winter peak demand here) is used to calculate LLO. The duration of each loss of load, LLD, is also recorded. Expected energy not supplied, ENS, is recorded for each loss of load, calculated as $\mathrm{ENS} = \mathrm{LLO}_*\mathrm{LLD}$. The above-mentioned information is recorded whenever generation capacity is below demand, and is aggregated for each simulation year *i*.

A set of metrics, calculated by averaging over the results of *N* simulation years, are calculated to measure the reliability of the electricity network. Loss of load frequency per year

$$\mathrm{LOLF} = \frac{1}{N}\sum_{i=1}^{N}\mathrm{LLO}_i \tag{8}$$

loss of load expectation per year

$$\mathrm{LOLE} = \frac{1}{N}\sum_{i=1}^{N}\mathrm{LLD}_i \tag{9}$$

and ENS in MWh per year [49]

$$\mathrm{EENS} = \frac{1}{N}\sum_{i=1}^{N}\mathrm{ENS}_i. \tag{10}$$

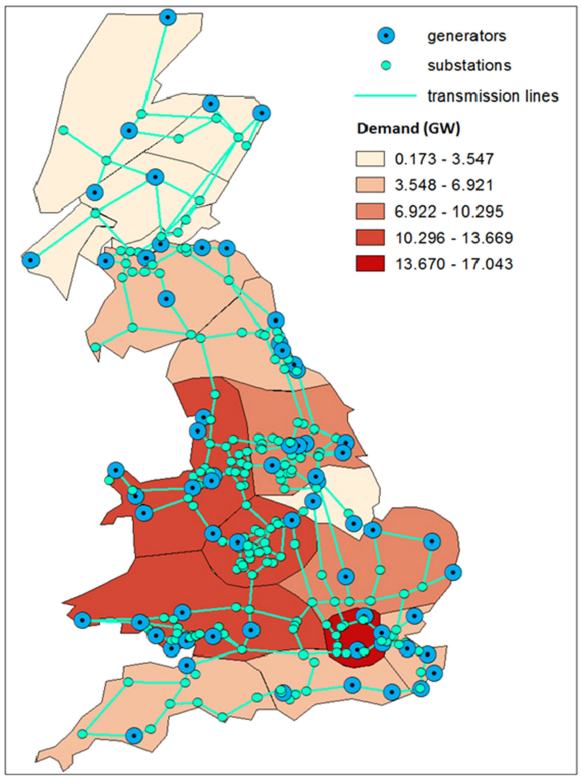

Fig. 7. Network representation of current NETS plotted on a backdrop of 17 regionalized electricity demand zones (winter peak demand of 2010).

IV. Case Study Application to National Electricity Transmission Network of the GB

A case study of the National Electricity Transmission System (NETS) of GB is used to demonstrate the methods described in Sections II and III. Possible network development pathways, under different future scenarios, are described in this section. The results of the storm resilience assessment of the NETS are reported in Section V.

A. Case Study Description

The NETS transmits power at high voltages (between 132 and 400 kV) to satisfy demand across GB. NETS has a generation capacity of 74.7 GW (from major generators), and the maximum recorded load for 2014/2015 was 52.5 GW, or around 70 per cent of the major generating capacity [50]. There is an average power flow of about 11 GW from the north to the south of GB across the NETS.

A network representation of the NETS was constructed using datasets obtained from [51]. To improve computational efficiency, power lines and cables have been straight lined; parallel overhead lines sharing the same towers have been defined as a single network link and are both considered to fail if one of supporting towers collapses; and small geographically colocated generation plants are aggregated into a single network node. The resultant network has 261 nodes, 335 links (each representing a pair of parallel lines). There are 65 generating nodes and 196 substation nodes. Fig. 7 shows the network plotted on a backdrop of 17 regionalized demand zones (winter peak demand of 2010 [52]).

B. Evolutionary Designs of NETS

Future network development scenarios are considered for the year 2050. By this time, the NETS is anticipated to have undergone significant change, with the introduction of a large amount of renewable generation, and the increase in electricity consumption from the electrification of heating and transport systems [4]. Although some commitments have been made (e.g., the planning and construction of around 25 GW of wind generation in Scotland and from coastal areas), there is still uncertainty on the longer term transition pathways for the future network [51].

In this study, a scenario-based approach is used to explore the possible transition pathways of the NETS. This provides a mechanism with which to relate network changes to the development of future infrastructure policies. A winter peak demand of around 95GW is anticipated by 2050 [51], [52] and, assuming that the system will maintain its load factor of 70%, this will require a generation capacity of $\sim$135.7 GW.

Four future scenarios have been designed to explore two major uncertainties related to future infrastructure policies and strategies: 1) the degree of centralized/distributed power generation and 2) the level of investment in network re-enforcement. Consideration of these two factors provides four different snapshots of the NETS in 2050 (shown in Fig. 8). All four scenarios incorporate the existing 25 GW commitments, but the shortfall of 45 GW is realized differently within each scenario.

Taking current NETS as input, the model described in Section II was used to generate future NETS. The regionalized demand distribution of 2050 [32], which is shown as the backdrop for the four example future NETS in Fig. 8, was used to formulate the demand density $\phi(a)$. The model was then parameterized with a primary objective of investigating the impact of the choice of infrastructure policies on network development. This was achieved by reconfiguring three parameters of the model, including the number of new generation nodes N_1, the number of substation nodes N_2, and the future electricity supply density $\psi(a)$. N_1 and N_2 were modeled as normally distributed integers with mean $\widehat{N_1}$ and $\widehat{N_2}$, and standard deviation σ_1 and σ_2, respectively. $\phi(a)$ was formulated depending on the centralized/distributed infrastructure policy choice, discussed as follows.

Other parameters, including γ, δ, and α, took fixed values obtained in our previous research [33] of $\gamma = 0.58$, $\delta = 0.58$, and $\alpha = 0.034$, respectively. Fixing these values ensures that the networks generated in all scenarios follow the node allocating and network wiring practices of existing NETS, also enabling us to focus on investigating only the influence introduced by infrastructure policies. The parameter settings for generating future NETS of four scenarios are listed in Table I.

Centralized generation encourages fewer, larger generation locations. The network growth model was configured with N_1 taking a small value, and having electricity supply density $\psi(a)$ set to be high values in the periphery of GB and being negatively correlated with demand density $\phi(a)$. This ensures that a small number of large generators (largely nuclear generators

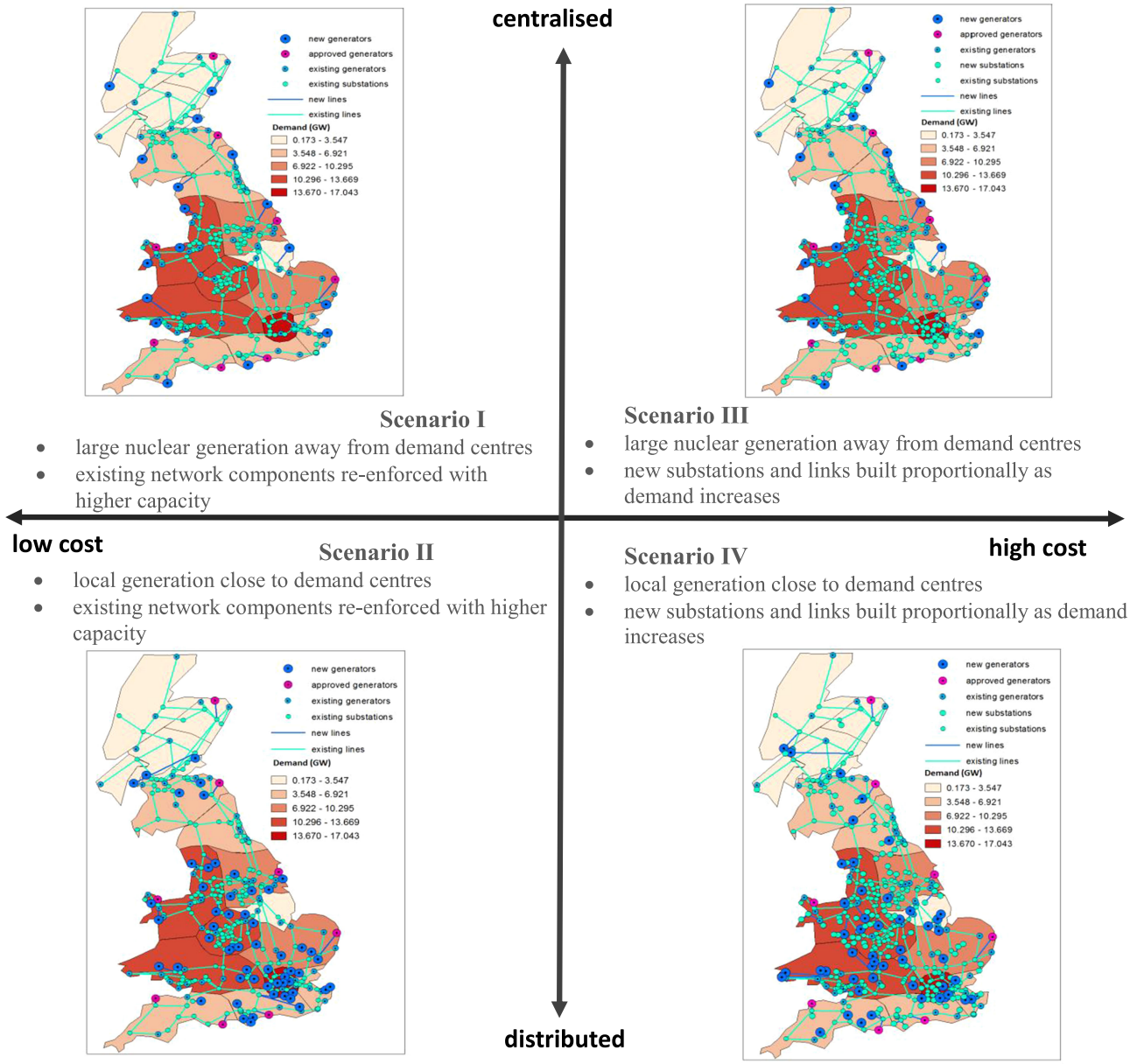

Fig. 8. Four infrastructure development scenarios and example future NETS which were generated with the model described in Section II using the parameter values listed in Table I, and with $\gamma = 0.58$, $\delta = 0.58$, and $\alpha = 0.034$. The networks are plotted on top of the regionalized demand distribution of year 2050 [32].

TABLE I
PARAMETER SETTINGS

scenario	$(\widehat{N_1},\ \sigma_1)$	$(\widehat{N_2},\ \sigma_2)$	$\psi(a)$
I	(15, 5)	(0, 0)	high density in the periphery of GB, $\psi(a)$ negatively correlated with $\phi(a)$
II	(50, 5)	(0, 0)	$\psi(a)$ positively correlated with $\phi(a)$
III	(15, 5)	(100, 20)	high density in the periphery of GB, $\psi(a)$ negatively correlated with $\phi(a)$
IV	(50, 5)	(100, 20)	$\psi(a)$ positively correlated with $\phi(a)$

according to [4]) will be constructed and located away from demand centers. Distributed generation prefers smaller generation sites close to demand centers, and the network growth model was configured with N_1 assigned a greater value and with $\psi(a)$ being positively correlated with $\phi(a)$. This ensured that new and small capacity generations were built and collocated with the demand. The number of generation nodes in a centralized case is set to be lower compared to the one in a distributed case.

High cost network plans accommodate increased demand by the building of new substations and transmission lines (the average number of new substation nodes was set to 100 in this case), and they were distributed proportionally to the demand distribution. Low cost network plan disincentivises any new build, but

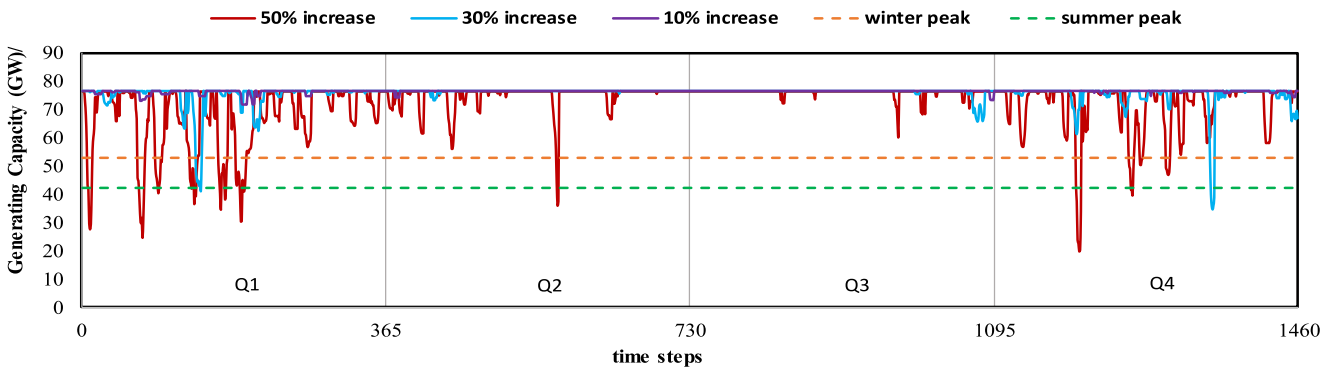

Fig. 9. Dynamic evolution of generating capacity of NETS at 6-h interval time steps for a randomly selected simulation year when wind storms increase their frequency and intensity by 10%, 30%, and 50%.

existing network components are upgraded with higher capacity to accommodate increased demand.

V. Storm Resilience Assessment of NETS Under Alternative Development Scenarios

The resilience of the present and future NETS was analyzed by simulating 100 years of wind storms at 6 hourly intervals at a 12 km × 12 km resolution using the method described in Section III. Unless otherwise specified, all results reported in this research were averaged over this time frame. Wind storms with increased intensity and frequency, incrementally up to 50% for each, were generated to explore the sensitivity of the metrics in (9) and (10) to possible changes in climate.

A. Baseline Study of the Present Network

The resilience of the present NETS was studied first. Fig. 9 shows a time-series of the NETS generation capacity, calculated at 6 hourly intervals. This shows that the NETS is resilient to storms at the current level of intensity and frequency, but this resilience will decrease if storms increase in intensity and frequency in future. Loss of load starts to occur if the intensity and frequency of wind storms increases by 5%–10%, and this accelerates rapidly with increasing wind intensities and frequencies. The frequency of large-scale loss of load increases dramatically when the increase of storm intensity and frequency is over 30%.

The system could collapse under a 50% increase of wind intensity and frequency as shown in Fig. 10, which plots the probability distribution of the capacity margin of NETS under different storm scenarios. Capacity margin is defined here as the difference between connected generations and winter peak demand. In the most severe case (50% increase of storm intensity and frequency), a shortfall of electricity of as much as 45 GW could occur, although this scenario has a low probability associated with it. This shortfall counts for 85% of winter peak demand (52.5 GW), and is greater than the summer peak demand (43 GW) of GB, indicating a probability of catastrophic failure of the whole system.

Increasing storm intensity and frequency have different effects on system performance, as shown in Fig. 11. Increasing storm intensity has the greater impact, with LOLF increasing exponentially with the increase rate of storm intensity. Increasing storm frequency has less impact, and a linear relationship

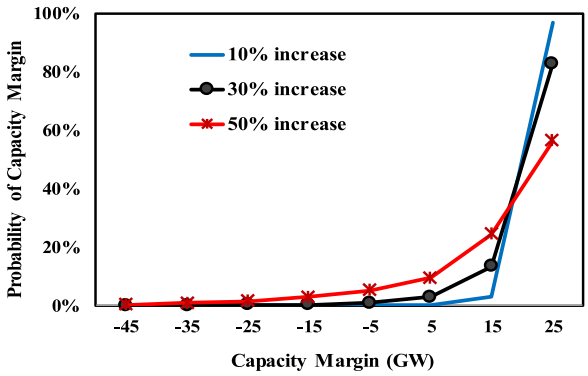

Fig. 10. Probability distribution of capacity margin of NETS when wind storms increase both frequency and intensity by 10%, 30%, and 50%.

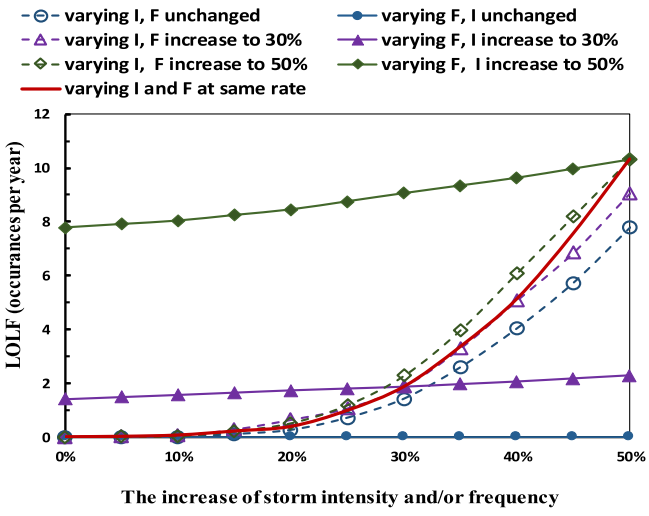

Fig. 11. LOLF (Loss of load occurrences per year) as a function of increasing rate of wind storm intensity and frequency, where *I* stands for wind intensity and *F* stands for wind frequency.

between LOLF and change rate was observed. Other resilience metrics, such as LOLD and EENS, exhibit similar relationships.

Analysis was also carried out to identify vulnerable network nodes and links of NETS. This was obtained by first calculating the number of failure occurrences for each network component

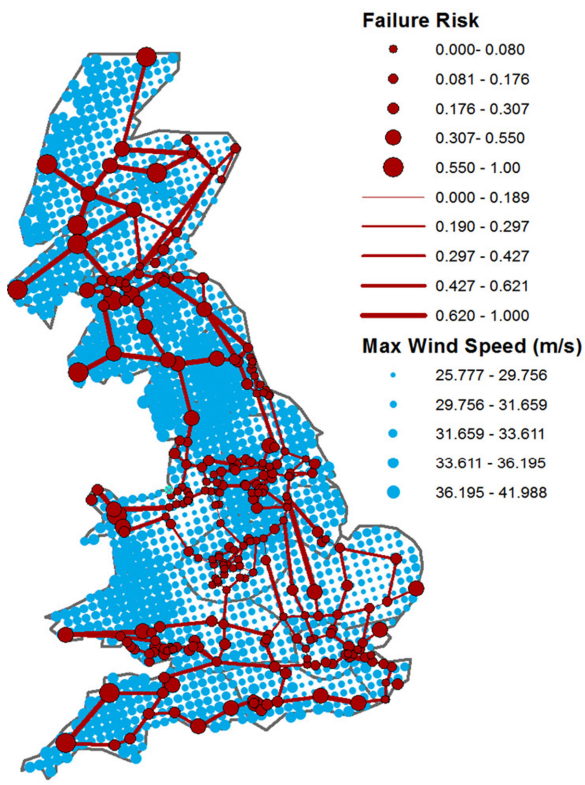

Fig. 12. Vulnerability map of network nodes/links of NETS, superimposed onto a map of the maximum wind speed from 100 years of simulated storms in each 12 × 12 km grid cell for the current climate.

under all-weather scenarios. The results were then normalized against that of the network component which experiences the highest number of failures. This generates a vulnerability index for each network component, in range [0,1], and the larger the value the more vulnerable the component. The results are plotted in Fig. 12, where the vulnerability map of NETS overlays the maximum wind speed (under current climate conditions). This shows a positive correlation between the failure probability of network components and the maximum wind speed in the simulation period. For example, failure probabilities are typically higher in northern and western coastal areas of GB. This explains the large-scale loss of load observed in simulations as there is a large quantity of power generation surplus in the north and coastal areas, and power typically flows from the north to the south. As there are currently only limited connections between the north and south, failure of these network components can severely constrain power transmission. Protecting and enhancing the reliability of these components are vital to securing power supply in GB.

B. Storm Resilience Analysis of Future NETS

This section analyses the reliability of the future NETS, with the aim to understand the implication of infrastructure policies on the climate resilience of the NETS. The network growth model (presented in Section II) was used to generate future NETS for scenarios I–IV (as described in Section IV). Results are presented in Fig. 13, which show the average from 100 future network realizations, each subjected to 100 years of wind storms.

The results show that infrastructure policies have significant implication for the long-term resilience of the NETS. While the networks of all four scenarios remain resilient to wind storms for the current climate, Fig. 13(a) shows that this resilience decreases as storm intensity and frequency increase. Loss of performance is most significant for scenario I, and least for scenario IV. Fig. 13(b) and (c) shows the variability of generation capacity and capacity margin under four scenarios. Networks of scenario IV demonstrate the lowest variability and hence best performance. Moreover, scenario IV is the only future scenario that shows an improvement in network resilience relative to the current configuration. For example, for an increase in storm intensity and frequency of 30%, LOLF increases by 148%, 116%, and 65% for scenarios I, II, and III, respectively, but drops to 76% for scenario IV.

The poor performance of scenario I networks is mainly due to the preference toward large capacity, centralized generations that are located at the extremities of the NETS, e.g., wind generation in the north and in coastal areas, and large nuclear generation in peripheral areas of GB. These are far from demand centers, and often at the locations of the most severe wind storms. Though networks under scenario II have generations close to demand, they also experience an overall decrease in performance compared to the present NETS. This is mainly due to the low-cost policy that disincentivises the construction of new substations and overhead line routes. Moreover, as the number of generation sites increases, the loss of a transmission line in this scenario becomes more likely to disconnect a generator than the present NETS.

Both scenarios III and IV invest in new substations and overhead line routes. This improves network connectivity, and generators have more paths to transport power. Failure of a transmission line is, therefore, less likely to disconnect a generator from the demand. Scenario IV networks perform better than the current NETS because a decentralized policy allocates small generators close to demand centers. This both reduces the likelihood of generation disconnection, as high demand areas are typically in less storm intensive regions of GB, and also deceases the impacts of a generation disconnection because a distributed policy encourages use of smaller capacity generation and so services fewer people.

Putting our results into context, we make the following observations. First, due to a lack of empirical data to define some parameters, such as $\beta\gamma$ in (5) and $\widehat{TTR}_{\mathrm{norm}}$ in (6), recommended or estimated values have been adopted. Second, large uncertainties surround the modeling of climate change scenarios. This is particularly true for wind extremes, where the problem is compounded by limitations of the models in reproducing current wind extremes and the coarse spatial resolution of climate models relative to topographic variability. Finally, to reduce computational overhead and complexity, a few simplifications have been made. For example, the complex geometries of power lines have been simplified as straight lines, parallel lines are represented as single lines and assumed to experience same load during extreme weather events, whilst the network components are assumed to have no capacity restrictions. These assumptions to manage uncertainties in available data are

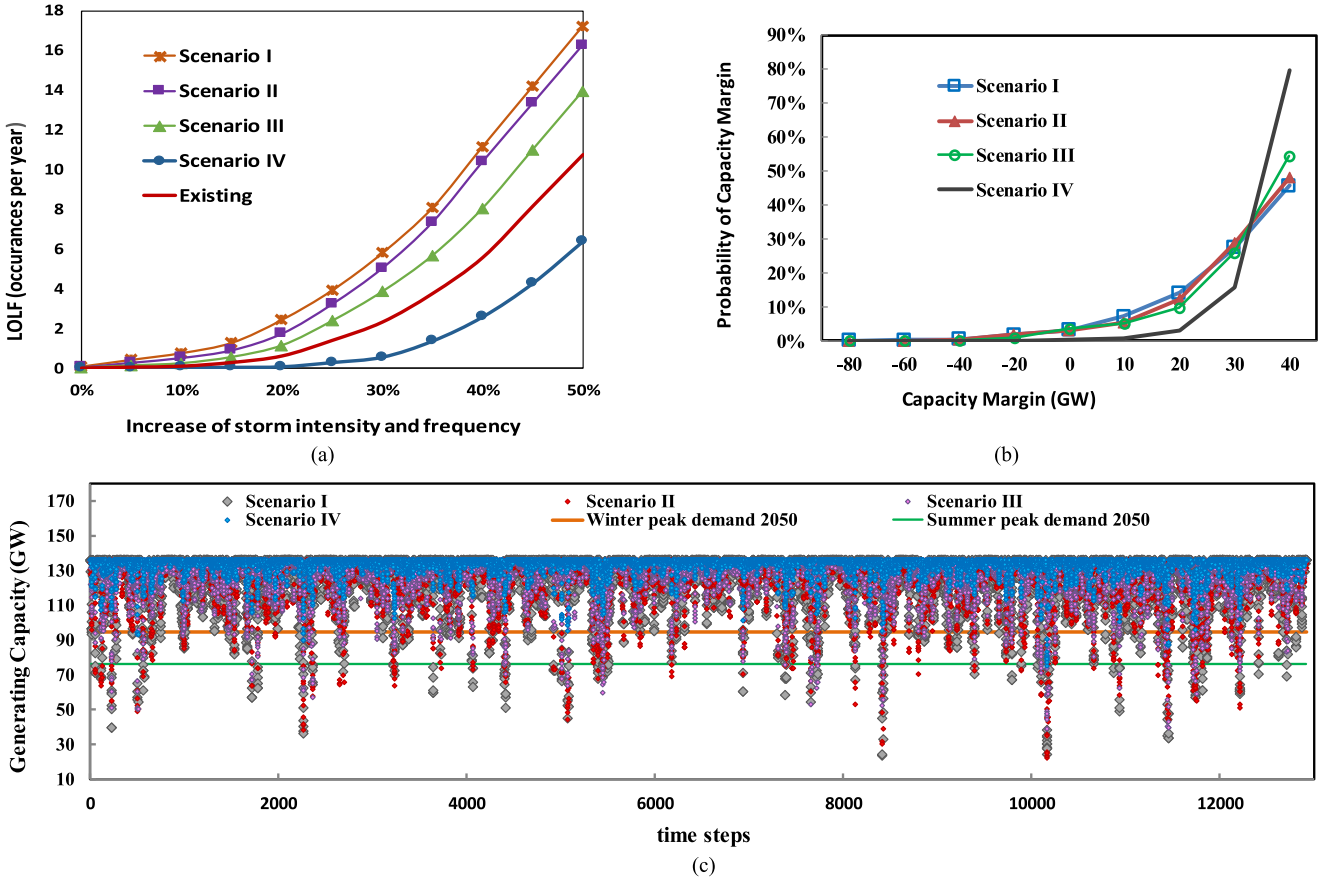

Fig. 13. Resilience analysis of future NETS under alternative infrastructure development policies and scenarios (a) LOLF measure of future NETS as a function of wind storm intensity and frequency increase, and results are compared against that of present NETS (red curve), (b) distribution of capacity margin of future NETS under wind storms with 30% increase of storm intensity and frequency, and (c) dynamic evolution of generating capacity of future NETS under four scenarios with 30% increase of storm intensity and frequency (here, we only plot the results for the time steps when max storm speed exceeds 20 m/s).

necessary for systems scale analysis. Since these were used and treated consistently in our simulations, the observations and results generated in this research provide meaningful insights into the trade-offs and benefits of infrastructure policy choices for the scenarios considered, and in relating network changes to the development of future policies and strategies.

VI. Conclusion and Future Research

Electricity networks are undergoing unprecedented change in response to the pressures of rising demand and emissions reduction targets. Networks are also threatened by projected changes to the intensity and frequency of weather hazards. To address these multiple and concurrent challenges, we have developed a system-level modeling framework for assessing network resilience. The framework has been demonstrated through application to the electricity transmission network of GB.

The analysis shows that infrastructure policies critically shape the long-term spatial configuration of electricity networks. This has profound impacts on system resilience. Four policy scenarios were tested, based on the degree of centralization of generation and the investment costs. Only scenario IV increased system resilience relative to the current system as it had the combined effects of reducing the impact of loss of generators and increasing network redundancy. Currently, there is a surplus of electricity generation in the north of GB, providing power to large demand centers in the south and the midlands. The lines between the north and south are already near capacity, though additional connectors are planned. Under scenarios I and III, with more centralized generation, the impacts of a wind storm disrupting these north–south connections are far greater than for the current network. In these scenarios, centralized generation should be coupled with improved network connectivity to enhance, or maintain, present levels of resilience. Our analysis further shows that under the current climate the transmission network is resilient to wind storm; however, under all future network scenarios, a slight increase of 10% in intensity and frequency would impact on network resilience. Further increases in intensity would exponentially increase the impacts of disruption from extreme wind events.

The approach provides a useful means for communicating potential network risks to different stakeholders who are trying to address often conflicting social (e.g., security of supply), economic (e.g., network cost), and environmental (e.g., decarbonization) objectives. Moreover, the research highlights the value of using systems based approach for assessing the resilience of infrastructure networks. Although the focus here has been on electricity systems and storm hazards, the approach

could be used to assess the resilience of other complex infrastructure systems, and other climate-related hazards. Finally, further development will consider the climate resilience of systems-of-systems, e.g., the impacts of climate hazards on a coupled electricity and transport network.

ACKNOWLEDGMENT

The authors would like to thank L. Manning and C. Pickering for their input on the wind modeling and fragility modeling in this research.

REFERENCES

[1] HM Treasury, "National infrastructure plan 2014," HM Treasury, London, U.K., 2010.
[2] G. Fu, D. Dawson, M. Khoury, and S. Bullock, "Interdependent networks: Vulnerability analysis and strategies to limit cascading failure," *Eur. Phys. J. B*, vol. 87, no. 7, 2014, Art. no. 148.
[3] A. Otto *et al.*, "A quantified system-of-systems modeling framework for robust national infrastructure planning," *IEEE Syst. J.*, vol. 10, no. 2, pp. 385–396, Jun. 2016.
[4] Nat. Grid, "Future energy scenarios," Nat. Grid, Warwick, U.K., 2016.
[5] IPCC, "Managing the risks of extreme events and disasters to advance climate change adaptation—Special report of the intergovernmental panel on climate change," Cambridge Univ., Cambridge, U.K., 2012.
[6] J. Murphy *et al.*, "UK climate projections science report: Climate change projections," Met Office Hadley Centre, Exeter, U.K., 2009.
[7] M. Beniston *et al.*, "Future extreme events in European climate: An exploration of regional climate model projections," *Clim. Change*, vol. 81, pp. 71–95, May 2007.
[8] H. Füssel and A. Jol, "Climate change, impacts and vulnerability in Europe 2012 an indicator-based report," Eur. Environ. Agency, Luxembourg, Publications Office Eur. Union, EEA Rep. No. 12/2012, 2012.
[9] D. M. Ward, "The effect of weather on grid systems and the reliability of electricity supply," *Clim. Change*, vol. 121, no. 1, pp. 103–113, Nov. 2013.
[10] P. Hines, J. Apt, and S. Talukdar, "Large blackouts in North America: Historical trends and policy implications," *Energy Policy*, vol. 37, pp. 5249–5259, 2009.
[11] L. McColl *et al.*, "Assessing the potential impact of climate change on the UK's electricity network," *Clim. Change*, vol. 115, nos. 3–4, pp. 821–835, Dec. 2012.
[12] Defra, "The CCRA evidence report: UK 2017 climate change risk assessment," Dept. Environ., Food Rural Affairs, London, U.K., 2016.
[13] D. E. Newman, B. A. Carreras, V. E. Lynch, and I. Dobson, "Exploring complex systems aspects of blackout risk and mitigation," *IEEE Trans. Rel.*, vol. 60, no. 1, pp. 134–143, Mar. 2011.
[14] B. A. Carreras, V. E. Lynch, I. Dobson, and D. E. Newman, "Complex dynamics of blackouts in power transmission systems," *Chaos*, vol. 14, no. 3, pp. 643–652, Sep. 2004.
[15] I. Dobson, B. A. Carreras, V. E. Lynch, and D. E. Newman, "Complex systems analysis of series of blackouts: Cascading failure, critical points, and self-organization," *Chaos*, vol. 17, no. 2, Jun. 2007, Art. no. 026103.
[16] P. Wang and R. Billinton, "Reliability cost/worth assessment of distribution systems incorporating time-varying weather conditions and restoration resources," *IEEE Trans. Power Del.*, vol. 17, no. 1, pp. 260–265, Jan. 2002.
[17] L. Chang and Z. G. Wu, "Performance and reliability of electrical power grids under cascading failures," *Int. J. Electr. Power*, vol. 33, no. 8, pp. 1410–1419, Oct. 2011.
[18] S. Chandramowli and F. Felder, "Impact of climate change on electricity systems and markets—A review of models and forecasts," *Sustain. Energy Technol. Assess.*, vol. 5, pp. 62–74, 2014.
[19] M. T. H. van Vliet *et al.*, "Vulnerability of US and European electricity supply to climate change," *Nat. Clim. Change*, vol. 2, no. 9, pp. 676–681, Sep. 2012.
[20] L. A. Bollinger and G. P. J. Dijkema, "Evaluating infrastructure resilience to extreme weather—The case of the Dutch electricity transmission network," *Eur. J. Transp. Infrastruct.*, vol. 16, no. 1, pp. 214–239, Jan. 2016.
[21] Y. J. Zhou, A. Pahwa, and S. S. Yang, "Modeling weather-related failures of overhead distribution lines," *IEEE Trans. Power Syst.*, vol. 21, no. 4, pp. 1683–1690, Nov. 2006.
[22] K. Alvehag and L. Soder, "A reliability model for distribution systems incorporating seasonal variations in severe weather," *IEEE Trans. Power Del.*, vol. 26, no. 2, pp. 910–919, Apr. 2011.
[23] D. Reed, K. Kapur, and R. Christie, "Methodology for assessing the resilience of networked infrastructure," *IEEE Syst. J.*, vol. 3, no. 2, pp. 174–180, Jun. 2009.
[24] D. Reed, M. Powell, and J. Westerman, " Energy infrastructure damage analysis for hurricane Rita," *Nat. Hazards Rev.*, vol. 11, no. 3, pp. 102–109, 2010.
[25] S. E. Chang, T. L. McDaniels, J. Mikawoz, and K. Peterson, "Infrastructure failure interdependencies in extreme events: Power outage consequences in the 1998 Ice Storm," *Nat. Hazards*, vol. 41, no. 2, pp. 337–358, May 2007.
[26] K. Murray and K. Bell, "Wind related faults on the GB transmission network," in *Proc. 13th Int. Conf. Probab. Methods Appl. Power Syst.*, Durham, U.K., 2014, pp. 1–6.
[27] E. Bompard, D. Wu, and F. Xue, "Structural vulnerability of power systems: A topological approach," *Electr. Power Syst. Res.*, vol. 81, no. 7, pp. 1334–1340, Jul. 2011.
[28] M. Panteli and P. Mancarella, "Modeling and evaluating the resilience of critical electrical power infrastructure to extreme weather events," *IEEE Syst. J.*, vol. 11, no. 3, pp. 1733–1742, Sep. 2017.
[29] R. Albert, I. Albert, and G. Nakarado, "Structural vulnerability of the north American power grid," *Phys. Rev. E, Stat. Phys. Plasmas Fluids Relat. Interdiscip. Top.*, vol. 69, no. 2, Feb. 2004, Art. no. 025103.
[30] S. Boccaletti *et al.*, "Complex networks: Structure and dynamics," *Phys. Rep.*, vol. 424, nos. 4–5, pp. 175–308, Feb. 2006.
[31] M. Newman, A. Barabasi, and D. Watts, *The Structure and Dynamics of Networks*, 1st ed. Princeton, NJ, USA: Princeton Univ. Press, 2006.
[32] R. N. Allan and R. Billinton, "Concepts of power-system reliability evaluation," *Int. J. Electr. Power*, vol. 10, no. 3, pp. 139–141, Jul. 1988.
[33] G. Fu, S. Wilkinson, and D. Dawson, "A spatial network model for civil infrastructure system development," *Comput.-Aided Civil Inf.*, vol. 31, no. 9, pp. 661–680, 2016.
[34] S. Wilkinson, H. Fowler, L. Manning, and S. Dunn, "Estimates of extreme wind speed used for the design of buildings," Newcastle Univ. Eur. Commission—ECLISE Deliverable 4.07 of Task T4.5, Newcastle upon Tyne, U.K., 2014.
[35] D. P. Dee *et al.*, "The ERA-Interim reanalysis: Configuration and performance of the data assimilation system," *Quart. J. Roy. Meteorol. Soc.*, vol. 137, no. 656, pp. 553–597, 2011.
[36] R. Hewston and S. R. Dorling, "An analysis of observed daily maximum wind gusts in the UK," *J. Wind Eng. Ind. Aerodyn.*, vol. 99, no. 8, pp. 845–856, 2011.
[37] G. Zappa *et al.*, "A multimodel assessment of future projections of north Atlantic and European extratropical cyclones in the CMIP5 climate models," *J. Clim.*, vol. 26, no. 16, pp. 5846–5862, 2013.
[38] F. Casciati and L. Faravelli, *Fragility Analysis of Complex Structural Systems*. Taunton, U.K.: Res. Stud. Press, 1991.
[39] R. J. Dawson and J. W. Hall, "Adaptive importance sampling for risk analysis of complex infrastructure systems," *Proc. Roy. Soc. Lond. A, Math.*, vol. 462, no. 2075, pp. 3343–3362, 2006.
[40] F. Cavalieri, P. Franchin, J. A. M. B. Cortes, and S. Tesfamariam, "Models for seismic vulnerability analysis of power networks: Comparative assessment," *Comput.-Aided Civil Inf.*, vol. 29, no. 8, pp. 590–607, Sep. 2014.
[41] Applied Technology Council, "Seismic performance assessment of buildings volume 1—Methodology," Fed. Emergency Manage. Agency, Washington, DC, USA, FEMA P-58-1, 2011.
[42] M. Panteli *et al.*, "Power system resilience to extreme weather: Fragility modelling, probabilistic impact assessment, and adaptation measures," *IEEE Trans. Power Syst.*, vol. 32, no. 5, pp. 3747–3757, Sep. 2017.
[43] P. Crucitti, V. Latora, and M. Marchiori, "A topological analysis of the Italian electric power grid," *Physica A*, vol. 338, nos. 1–2, pp. 92–97, Jul. 2004.
[44] M. Rosas-Casals, S. Valverde, and R. V. Sole, "Topological vulnerability of the European power grid under errors and attacks," *Int. J. Bifurcation Chaos*, vol. 17, no. 7, pp. 2465–2475, Jul. 2007.
[45] G. Pagani and M. Aiello, "The power grid as a complex network: A survey," *Physica A*, vol. 392, no. 11, pp. 2688–2700, 2013.
[46] R. Billinton and G. D. Singh, "Reliability assessment of transmission and distribution systems considering repair in adverse weather conditions," in *Proc. IEEE Can. Conf. Electr. Comput. Eng.*, Winnipeg, MB, Canada, 2002, pp. 88–93.

[47] R. Roy Billinton and R. N. Allan, *Reliability Evaluation of Power Systems*. New York, NY, USA: Plenum, 1996.
[48] R. Billinton, R. Ringlee, and A. J. Wood, *Power-System Reliability Calculations*. Cambridge, MA, USA: MIT, 1973.
[49] R. Billinton and W. Li, *Reliability Assessment of Power Systems Using Monte Carlo Methods*. New York, NY, USA: Plenum, 1994.
[50] Department of Energy and Climate Change, "Electricity: Chapter 5: Digest of united kingdom energy statistics 2015 (DUKES)," Dept. Energy Clim. Change, London, U.K., 2015.
[51] Nat. Grid, "Electricity ten year statement 2015," Nat. Grid, Warwick, U.K., 2015.
[52] F. R. Wood *et al.*, "The impact of climate change on UK energy demand," *Infrastruct. Asset Manage.*, vol. 2, no. 3, pp. 107–119, 2015.

Gaihua Fu received the B.Sc. degree in computer science from Inner Mongolia University, Hohhot, China, and the Ph.D. degree from Cardiff University, Cardiff, U.K.

She is currently an Information Architect with National Grid plc, Reading, U.K. Her research interests include complex system modeling, systems-of-systems modeling, infrastructure resilience assessment, infrastructure data modeling and integration, and knowledge management.

Sean Wilkinson received the M.Eng. degree in civil engineering in 1991, and the Ph.D. degree in earthquake engineering from the Queensland University of Technology, Brisbane, Qld., Australia, in 1997.

He is currently a Senior Lecturer in structural engineering with Newcastle University, Newcastle upon Tyne, U.K. His research interest focuses on building community resilience to natural hazards by understanding how critical infrastructure responds in a disaster.

Richard J. Dawson received the M.Eng. degree in civil engineering and Ph.D. degree in performance-based management of complex infrastructure systems from Bristol University, Bristol, U.K., in 1999 and 2003, respectively.

He is currently a Professor of earth systems engineering with Newcastle University, Newcastle upon Tyne, U.K., where one of his main research interests is the development of new approaches to analyses of environmental risks to infrastructure systems and the built environment.

Hayley J. Fowler received the B.A. degree in geography from Cambridge University, Oxford, U.K., in 1996, and M.Sc. degree in water resource systems engineering and Ph.D. degree in civil engineering from Newcastle University, Newcastle upon Tyne, U.K., in 1997 and 2000, respectively.

She is currently a Professor of climate change impacts with Newcastle University. Her research interests include the analysis of weather and climate extremes from observations and developing downscaling techniques to provide information for climate change impact studies.

Dr. Fowler was the recipient of the Wolfson-Royal Society Research Merit Award.

Chris Kilsby received the B.Sc. degree in physics from Sheffield University, Sheffield, U.K.

He then joined the Meteorological Office. He is currently a Professor of hydrology and climate change with Newcastle University, Newcastle upon Tyne, U.K., where his research interests include stochastic modeling of weather hazards and extremes and their impacts on infrastructure systems.

Mathaios Panteli (S'09–M'13) received the M.Eng. degree in electrical and computer engineering from Aristotle University, Thessaloniki, Greece, in 2009, and the Ph.D. degree in electrical power engineering from the University of Manchester, Manchester, U.K., in 2013.

He is currently a Lecturer with the Power and Energy Division, University of Manchester. His main research interests include analysis and prevention of power system blackouts and risk and resilience assessment of power systems.

Pierluigi Mancarella (M'08–SM'14) received the Ph.D. degree in electrical power systems from the Politecnico di Torino, Turin, Italy, in 2006.

He is currently a Reader in future energy networks with the Electrical Energy and Power Systems Group, University of Manchester, Manchester, U.K. His research interests include multi-energy systems, business models for smart grid technologies, energy system investment under uncertainty, and risk and resilience of future network infrastructure.